SAE International

2013-01-0762
Published 04/08/2013
doi:10.4271/2013-01-0762
saetransaf.saejournals.org

# Repeatability of a Small Overlap and an Oblique Moving Deformable Barrier Test Procedure

James Saunders and Daniel Parent
NHTSA

**ABSTRACT**

NHTSA has developed two different moving deformable barrier-to-vehicle test procedures to assess the vehicle and occupant response in narrow overlap motor vehicle crashes. An assessment of test repeatability is one of the requirements necessary to accept the test procedure as viable. Previous methodologies, coefficient of variation (CV) and similarity analysis were developed to assess the repeatability of vehicle and occupant response in motor vehicle crash tests for full frontal and 40% overlap tests procedures. These will be used for this assessment.

Three repeat tests were performed in each test procedure, with all other factors held constant: vehicles of the same make, model, and model year; moving deformable barriers of the same mass, velocity, and barrier face properties; and the same occupant - a THOR 50th percentile adult male in the driver's seat. In general, for this one vehicle make and model the repeatability of both vehicle and occupant response metrics were good for both test modes. In isolated cases, differences in occupant response resulted from the timing of side curtain air bag deployment.

**CITATION:** Saunders, J. and Parent, D., "Repeatability of a Small Overlap and an Oblique Moving Deformable Barrier Test Procedure," *SAE Int. J. Trans. Safety* 1(2):2013, doi:10.4271/2013-01-0762.

## INTRODUCTION

Saunders et al, 2012 [1] performed paired vehicle test in both "Small Overlap Impact" (SOI) and "Offset Oblique" (Oblique) test procedures with vehicles that were redesigned or introduced in 2010 and 2011. Most of these vehicles received highest ratings in current US consumer rating systems. Saunders et al, 2012 [1] demonstrated that even though these vehicles had good ratings in consumer information crash tests and were newly designed, there still exists potential for vehicle design improvements that could mitigate real-world injuries and fatalities in the both of these crash types.

A next step is to make sure these test procedures are repeatable. Meyerson et al, 1996 [2] reported on repeat tests of five vehicles in the 64 kph, 40 percent offset deformable fixed barrier test. Meyerson deemed this test procedure repeatable because the ratings of the vehicles did not change between the paired tests.

This paper presents the analysis of repeated 2011 Chevrolet Cruze tests, three each in the SOI and Oblique test modes, to assess the repeatability of these procedures. The paper uses established criteria for evaluating repeatability in comparing these two test procedures to repeatability in 56 kph full frontal and the 40 percent offset deformable barrier (ODB) test procedures with model year vehicles greater than 1999.

## METHODOLOGY

### Test Setup

This section describes the SOI and Oblique test procedures, as well as the methodology for presentation and analysis of the vehicle and occupant response. Figure 1 shows the general test setup for both test modes. The general procedure is to mark the overlap on the target vehicle (width excludes mirrors and door handle) and then position the stationary target at the desired angle. Once this is achieved, the outer edge of research moving deformable barrier (RMDB) is aligned with the overlap mark on the target vehicle. Table 1 shows the test parameters for both the SOI and Oblique test procedures.

Saunders et al, 2012 [1] described the reasoning for the design of the RMDB. It should be noted that the design characteristics (i.e. frontal stiffness) of the RMDB were not developed to match a specific or even an average passenger car, but were developed to address the issues observed when using the FMVSS No. 214 MDB for this testing. Figure 2 shows the basic dimensions and properties of the RMDB. The total weight of the barrier is 2486 kg (5481 lbs).

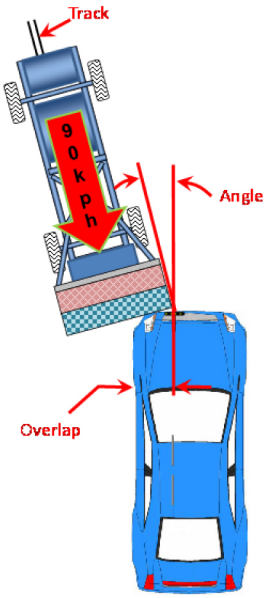


***Figure 1. Test configuration***

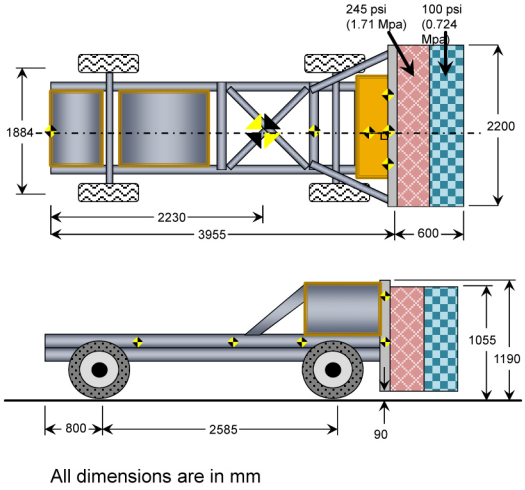


***Figure 2. Dimensions of the RMDB***

***Table 1. Setup parameters for SOI and Oblique test procedure***

| Test Type | Overlap (%) | Angle (degrees) | RMDB Closing Speed (kph/mph) |
|---|---|---|---|
| SOI | 20 | 7 | 90/56 |
| Oblique | 35 | 15 | 90/56 |

## Vehicle Parameters

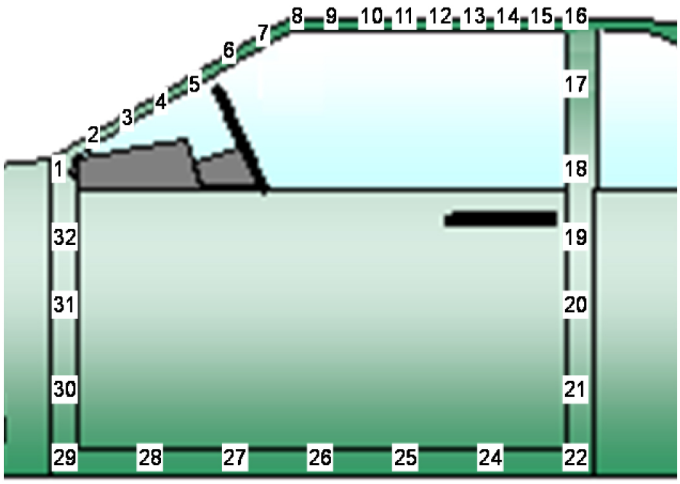


***Figure 3. Door profile measurement points***

This section describes the vehicle parameters and responses used for repeatability analysis:

**1.** The y and z distance from the target point. If y is positive it means the actual overlap was less than the calculated overlap.

**2.** 6 points on the bumper beam were recorded pre and post-test (see Appendix A for procedure to locate these points)

**3.** Door profile (DP) points (Figure 3) (see Appendix B for procedure to locate these points)

**4.** Interior intrusions points (Figure 4) (see Appendix C for procedure to locate these points):

**a.** Toepan points: points A2, B2, C2, D2 are used for this analysis

**b.** Left and right instrument panel (IP)

**c.** Steering wheel

**5.** Vehicle accelerations and velocities

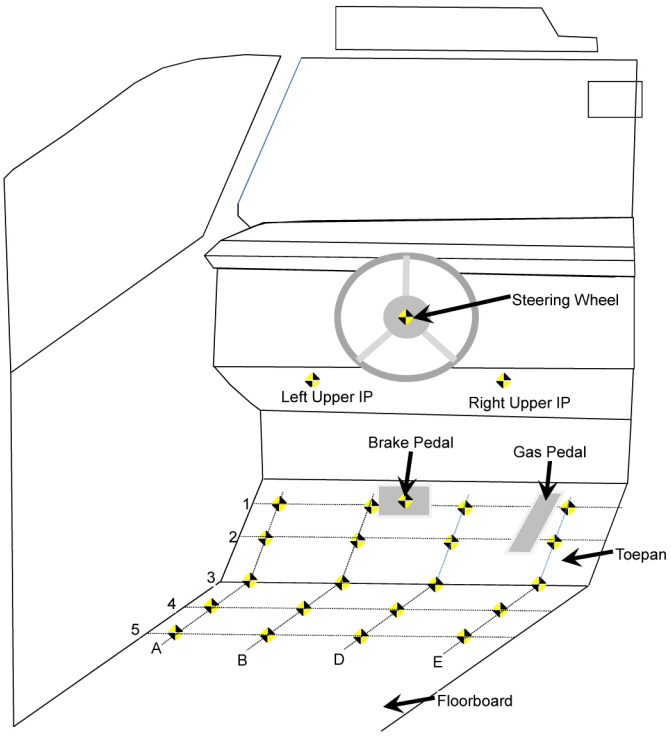


***Figure 4. Interior intrusion points***

## Occupant Response Assessment

In the SOI and Oblique RMDB tests, a Test Device for Human Occupant Restraint (THOR) 50$^{th}$ percentile male anthropomorphic test device (ATD) was positioned in the driver's seat. The THOR ATD used in the RMDB tests represents the Mod Kit build level [1].

While injury risk functions specific to the THOR hardware have not yet been developed [1], provisional injury assessment reference values have been developed for several body regions. To assess head injury risk, the head injury criterion ($HIC_{15}$ and $HIC_{36}$ results are both presented) is assumed to be applicable to THOR, since the design requirements for the mass, moment of inertia, and biomechanical response characteristics mirror that of the Hybrid III for which HIC is traditionally applied. The Injury Assessment Reference Values (IARVs) for $HIC_{15}$ and $HIC_{36}$ are 700 and 1000 [4]. The rotational brain injury criterion (BRIC) is implemented with critical values of 63.5 rad/s and 19,501 rad/s$^2$ [1], and the BRIC IARV is 0.89 [5]. For the neck, cervical spine axial load tolerance values of 2520 Newtons (N) in tension and 3640 N in compression [6]. Injury assessment reference values have not yet been determined for THOR chest deflection or 3-millisecond clip acceleration, so the Hybrid III IARVs of 63 millimeters and 60 g [4] are used for the purposes of this analysis. The fracture tolerance of a human hip under neutral loading through the knee was determined to be 4560 N [7]; adjusting for the difference in load transfer between the THOR dummy and human subjects, the associated load measured at the THOR acetabulum would be 3,316 N [8]. The IARV for the human femur in axial compressive load is 9,040 N [9]. Since the THOR femur was designed to meet the human response in axial compression, this IARV can be applied directly [3]. Lower extremity injury risk was assessed using the Revised Tibia Index, for which the IARV of 1.16 [9].

## Repeatability

To determine repeatability of these two test procedures, three tests of 2011 Chevrolet Cruze were performed in each procedure. Table 2 shows the NHTSA test numbers and the naming convention used throughout the paper.

***Table 2. Name of each test throughout the paper and NHTSA test number***

| Test Type | Name | NHTSA Test |
|---|---|---|
| SOI | SOI_1 | 7432* |
| | SOI_2 | 7773 |
| | SOI_3 | 7867 |
| Oblique | Oblique_1 | 7431* |
| | Oblique_2 | 7852 |
| | Oblique_3 | 7851 |

* Vehicle purchased with automatic transmission

### *Coefficient of Variation*

Coefficient of Variation (CV) is calculated (Eqn. 1) by dividing the standard deviation (Eqn. 2) of the test measurements, either a peak value or an injury assessment value (IAV), by the mean (Eqn. 3) of the given measurement values for each test in the group. The population standard deviation is used here since only the values in each group are being considered, not a projection on a greater population.

$$CV = \frac{\sigma}{\mu} \times 100\% \qquad \textit{Eq. 1}$$

$$\sigma = \sqrt{\frac{\sum (x-\mu)^2}{n}} \qquad \textit{Eq. 2}$$

$$\mu = \frac{1}{n}\sum x$$

*Eq. 3*

# RESULTS: VEHICLE RESPONSE

The section describes the vehicle response parameters and vehicle responses that are compared to determine the repeatability of the SOI and Oblique test procedures. The vehicle parameters include the actual overlap of the test (target point location), how the vehicle crushes and/or intrudes, and the acceleration/velocity of the vehicle.

Figure 5 shows that the RMDB impacted the desired target within 25 mm for the 6 tests performed. Figure 6 (a) and Figure 6 (b) shows the bumper beam crush for SOI and Oblique test procedure, respectively. It can be seen from Figure 6 (a) that SOI_1 had 129 mm difference in the x-direction when compared to SOI_2 and SOI_3. SOI_2 and SOI_3 had similar x-direction crush. Figure 6 (b) shows the oblique bumper crush was similar for each test. The max x-direction difference was only 58 mm.

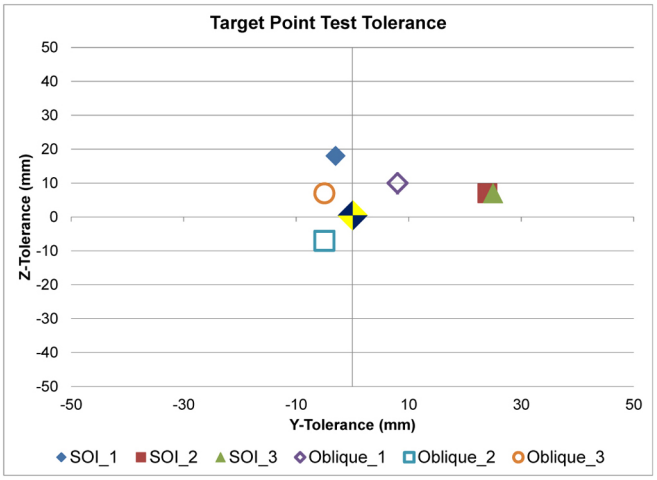


***Figure 5. Distance from target point***

Figure 7 (a) and Figure 7 (b) shows that the door profile was similar for both the SOI and Oblique test procedure. When looking at the lower rocker panel the max difference in the x-direction for the SOI tests was 52 mm and 59 mm for the oblique tests.

Figure 8 (a) and Figure 8 (b) show row 2 of the toepan x, y, and z intrusions for SOI and Oblique, respectively. Figure 8 (a) shows that SOI_3 had the highest intrusion in the X-direction and SOI_1 had the highest intrusion in the Z-direction. Figure 8 (b) shows Obique_1 had the highest intrusion in x, y, and z direction. The max difference for the SOI procedure occurred at A2Z and was 97 mm, whereas the max difference was 14 mm for the Oblique procedure.

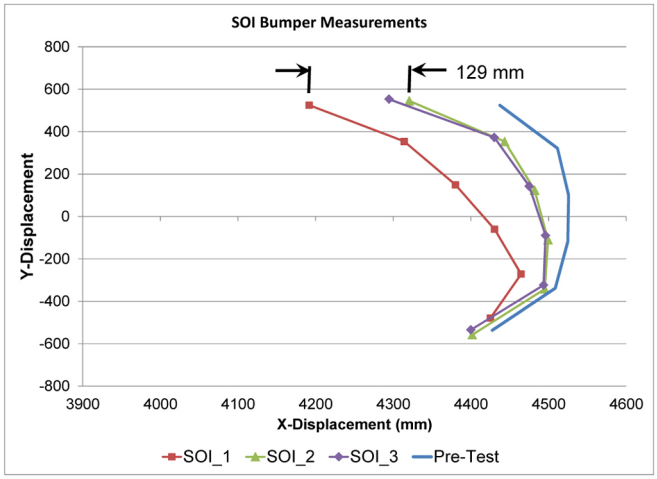


(a)

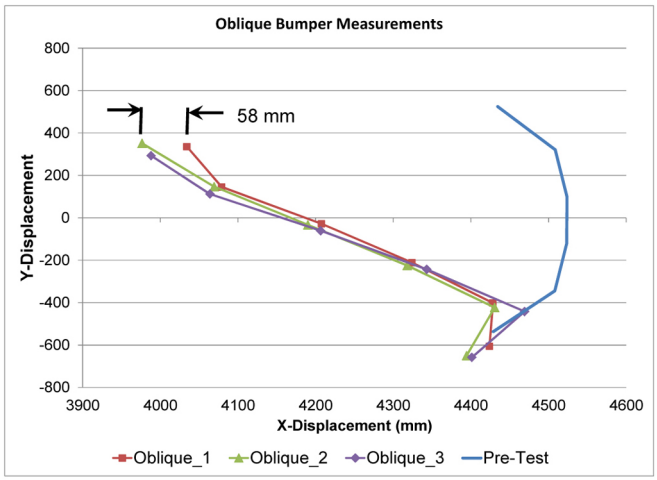


(b)

***Figure 6. Bumper crush***

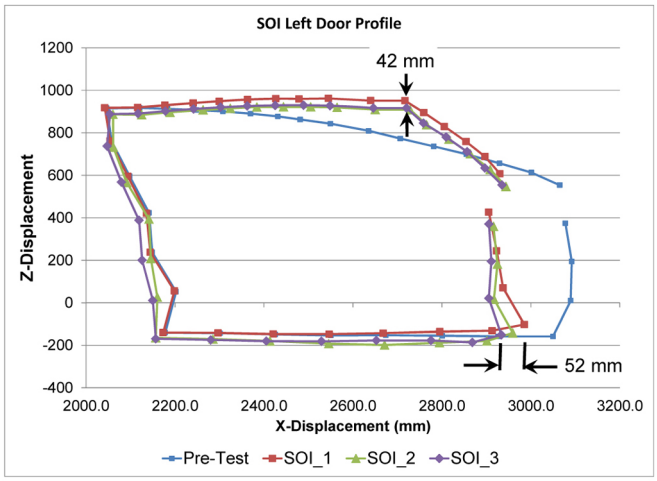


(a)

***Figure 7. Left door profile***

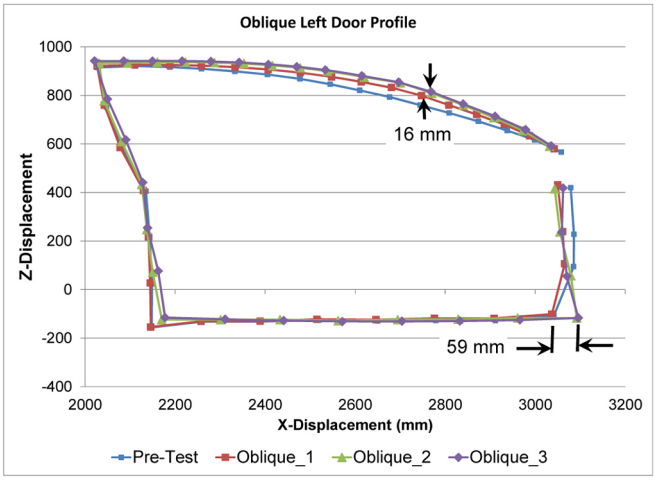


(b)

***Figure 7. (cont.) Left door profile***

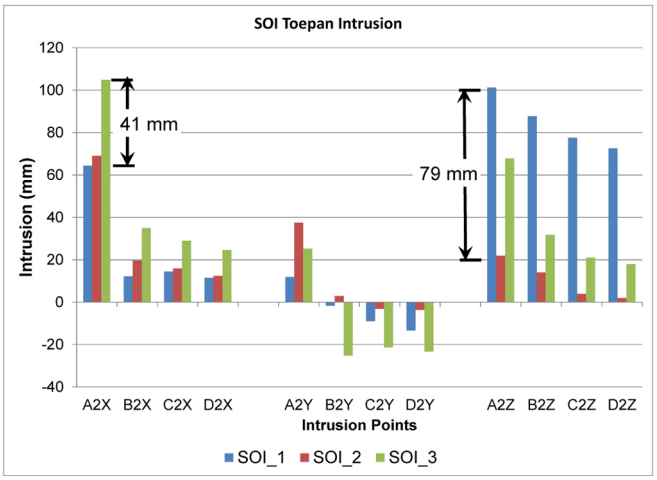


(a)

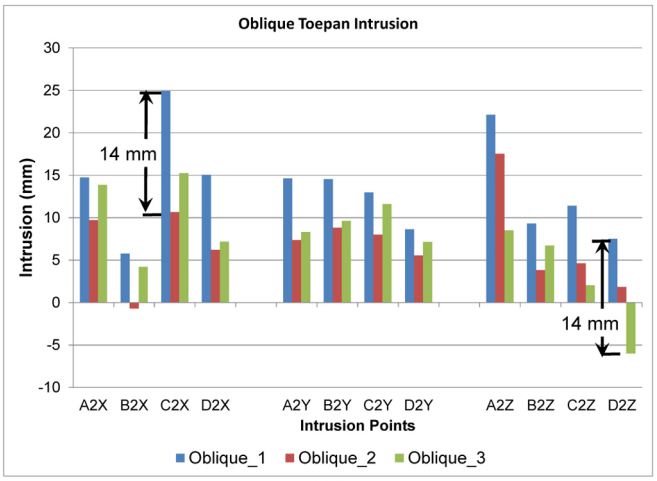


(b)

***Figure 8. Toepan row 2 x, y, and z difference in intrusion pre and post-test***

Figure 9 shows the x, y, and z intrusions for the left and right IP and the SW. It should be noted that the Z intrusion for the SW was flipped for graphical purposes. The X-direction intrusions were similar for both the left and right IP and the SW for both SOI and Oblique procedures (Figure 9 (a) and Figure 9(b)). The Z-direction intrusion for the left and right IP and SW showed the most variability for the SOI procedure.

Figure 10(a) shows that the left rear sill X-direction acceleration had similar shape and timing of peak Gs. Figure 10(b) shows that the Oblique test procedure had similar shape, but different timing of peak Gs. The difference between the Peak Gs and the CV for SOI was 6.6 Gs and 7.8 percent and 4.8 Gs and 7.3 percent for Oblique.

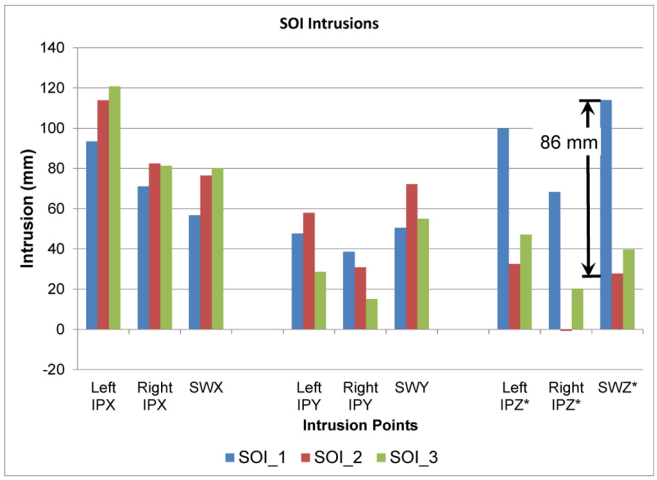


(a)

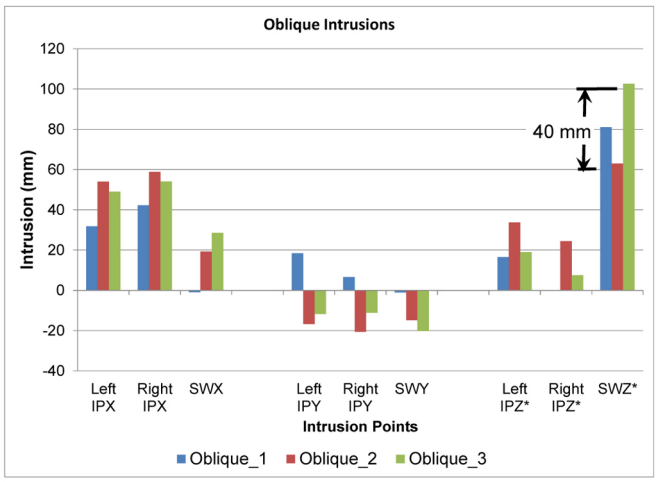


(b)

***Figure 9. IP and SW x, y, and z difference in intrusion pre and post-test***

Figure 11 (a) and Figure 11 (b) shows that both SOI and Oblique have similar velocity traces. The range in peak change in velocity (delta-V or DV) was approximately 2 kph

at 150 ms for both procedures and the CV was approximately 2 percent for both procedures.

Figure 12(a) and Figure 12 (b) show the left rear sill Y-direction acceleration. For both procedures the shape of the curves are similar. The difference in the Peak Gs for the SOI procedure was 2.7 Gs and the CV was 8.7 percent. The Oblique procedure difference in Peak Gs was 5.7 Gs and the CV was 13.8 percent.

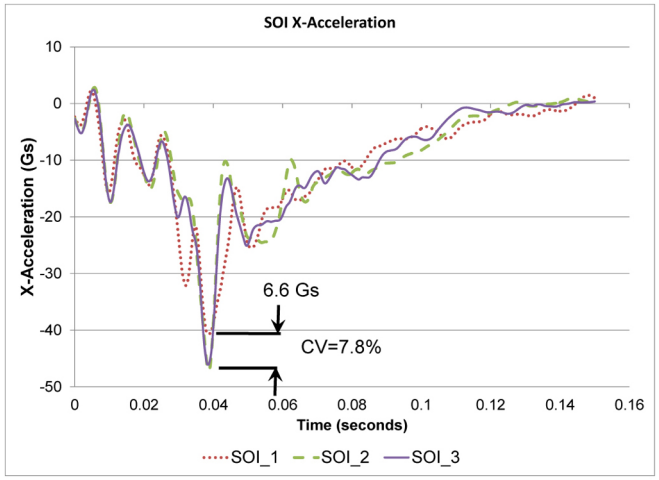


(a)

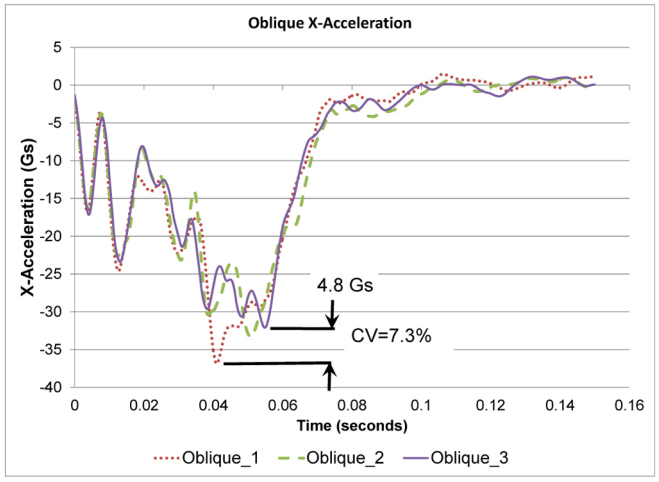


(b)

***Figure 10. Left rear sill x-acceleration***

Figure 13 (a) shows similar Y-direction velocity traces for the SOI procedure except from 60 to 80 ms. At 150 ms, the range DV was 3 kph and the CV was 8.1 percent. Figure 13 (b) shows that the Y-direction velocity in Oblique_3 was similar to the other tests up to 50 ms and then continued to go higher. At 150 ms, the range in DV and the CV were 4 kph and 14.3 percent, respectively.

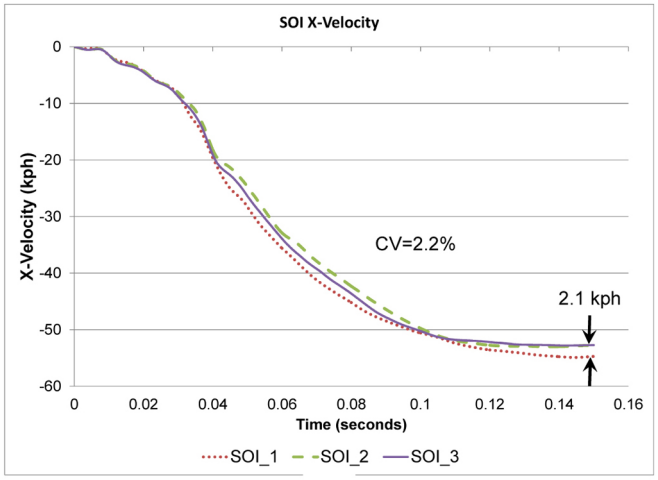


(a)

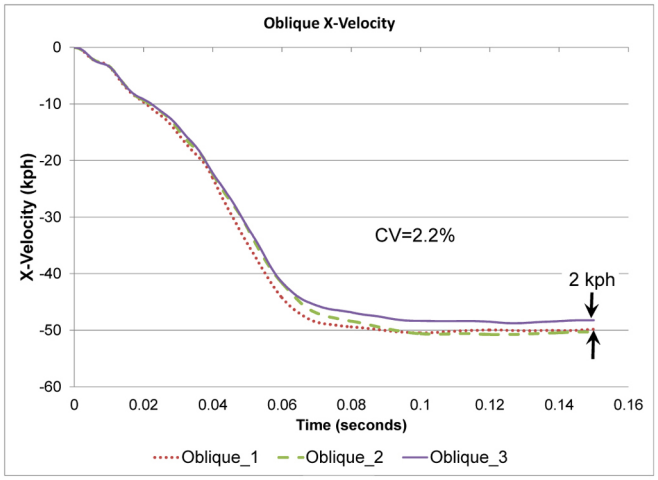


(b)

***Figure 11. Left rear sill x-velocity***

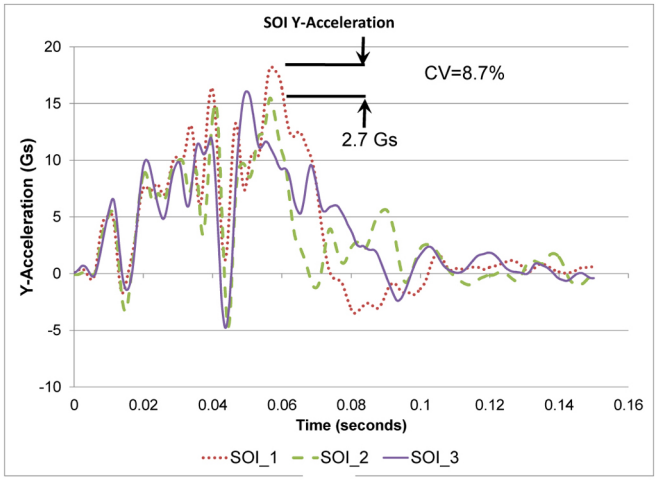


(a)

***Figure 12. Left rear sill y-acceleration***

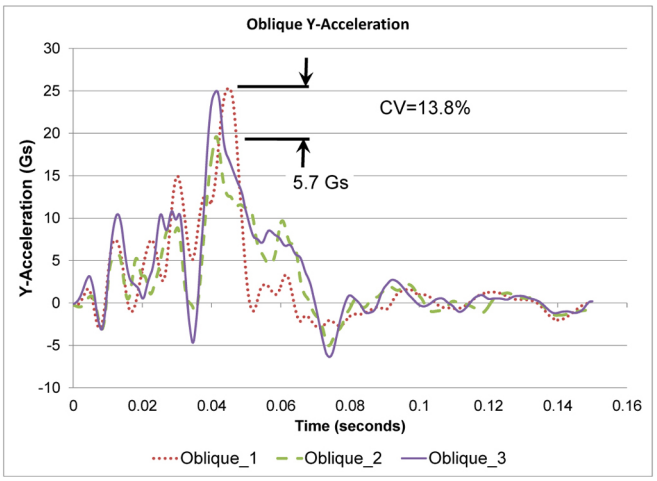


(b)

***Figure 12. (cont.) Left rear sill y-acceleration***

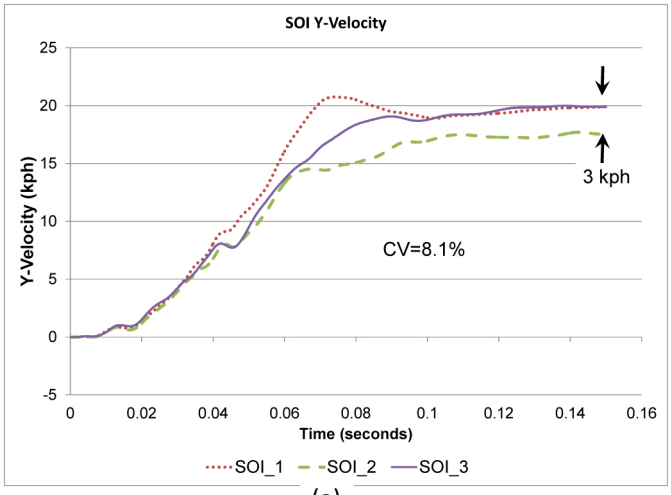


(a)

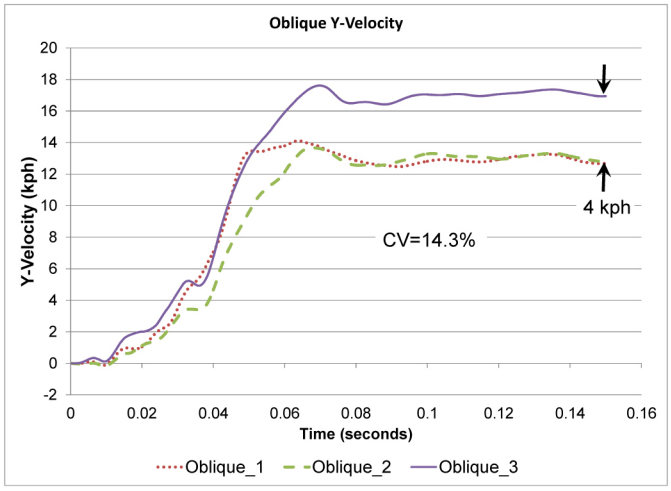


(b)

***Figure 13. Left rear sill y-velocity***

# RESULTS: OCCUPANT RESPONSE

Before the repeatability of occupant response can be assessed, the occupant environment must be evaluated for repeatability. There are three components to the assessment of occupant response repeatability: initial occupant position, acceleration pulse, and restraint performance.

## *Initial occupant position*

During the setup of the repeated tests, care was taken to ensure that a consistent position of the THOR ATD in the driver's seat was achieved for each test. Measurements were recorded using a digital three-dimensional spatial measurement device and compared with the first test in each condition during the positioning process. The occupant position was very repeatable in the X-Z plane (Figure 14), where the maximum test-to-test difference in the position of the Head CG marker was 9.4 millimeters in X-axis, and 16.2 millimeters in the Z-axis. There was greater variation in the Y-axis, where the position of the Head CG marker in SOI_1 was 28 millimeters inboard. The H-point marker was within 13.4 millimeters of the remaining tests, suggesting that the THOR ATD was leaning slightly inboard for this test.

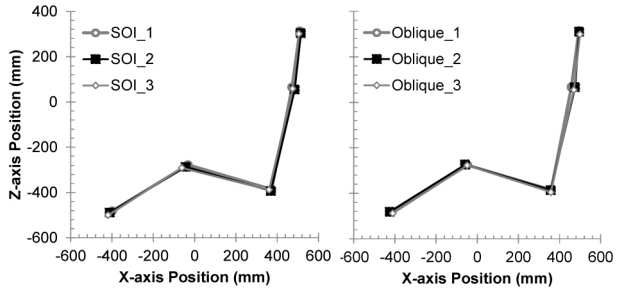


***Figure 14. Initial X-Z plane position of the head, shoulder, hip, knee, and ankle.***

## *Acceleration pulse*

As shown in Figure 10 and Figure 11, the acceleration pulses were generally similar in magnitude and shape, but showed some localized differences. For instance, the SOI peak vehicle acceleration in test SOI_1 showed very similar timing of the peak, but was lower in magnitude by 6.6 g. However, the peak accelerations tend to occur before the occupant is fully restrained by the lap and shoulder belt, so these localised differences are not realized in the occupant response.

## *Restraint performance*

There were several differences in restraint performance that may have contributed to differences in occupant response in the repeated SOI and Oblique tests. Although there were two exceptions, the restraint deployment times were consistently within two milliseconds for all tests (Table 3). One exception was test SOI_2, where the side curtain air bag deployed very late in the event after the point of peak head

excursion, and the seat-mounted torso air bag did not deploy. Another exception was test Oblique_2, where the side curtain and torso air bags deployed roughly ten milliseconds after they deployed in tests Oblique_1 and Oblique_3. Also of note is that the frontal air bag, knee bolster air bag, and retractor pretensioner trigger times occurred earlier in the event in the Oblique tests than in the SOI tests, though the side curtain and torso air bags deployed slightly later in the Oblique tests.

***Table 3. Deployment times, in milliseconds after impact, of the driver-side restraint systems***

| Deployment Time (ms) | SOI | | | Oblique | | |
|---|---|---|---|---|---|---|
| | 1 | 2 | 3 | 1 | 2 | 3 |
| Frontal AB | 36 | 38 | 38 | 20 | 20 | 20 |
| Side Curtain AB | 48 | 158 | 46 | 52 | 60 | 50 |
| Torso AB | 48 | NA | 46 | 52 | 60 | 50 |
| Knee Bolster AB | 36 | 38 | 38 | 20 | 20 | 20 |
| Retractor Pretensioner | 30 | 30 | 28 | 20 | 20 | 20 |

In terms of restraint loading of the occupant, the belt tension time-histories of the shoulder belt showed generally good repeatability (Figure 15), with peak loads showing CV % of 2% and 6% for the SOI and Oblique conditions, respectively. The lap belt tension time-histories were not as repeatable as those of the shoulder belt (Figure 16), with peak loads showing CV% of 13% and 10% for SOI and Oblique, respectively.

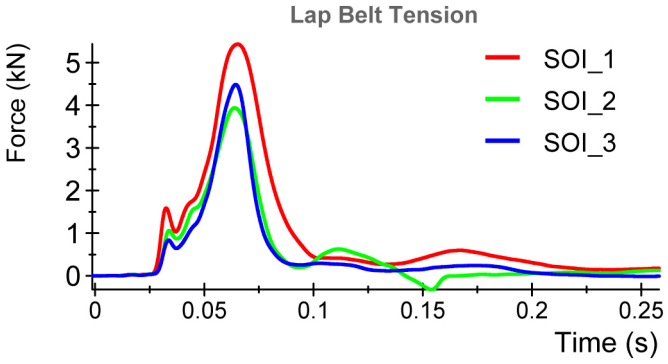


***Figure 15. Lap belt loads measured in the SOI condition.***

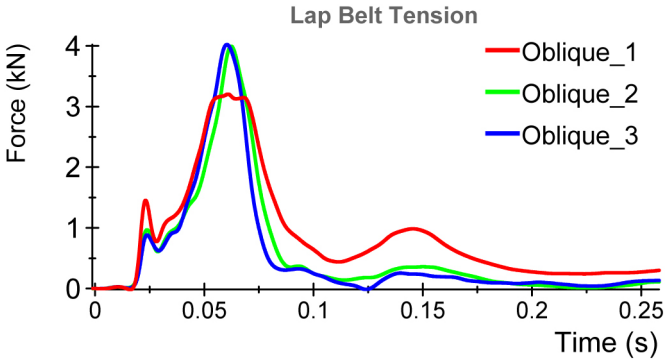


***Figure 16. Lap belt loads measured in the Oblique condition.***

## *Occupant kinematics*

In each of the two RMDB comparison groups, the response of the THOR ATD in the driver's seat demonstrated good qualitative repeatability in terms of gross kinematics as well as phase, magnitude, and shape of the kinetic responses.

There were localized differences in occupant kinematics, specifically motion of the head, which resulted from differences in restraint deployment. In the SOI_2 test, the side curtain air bag does not deploy until after the time of peak head excursion. Since the head is not restrained by the side curtain air bag, it rotates about its local Z-axis roughly 45 degrees more than the head does in the SOI_1 and SOI_3 tests (see bottom row of Figure 17).

As a result, the head acceleration (Figure 18) and angular velocity (Figure 19) time-histories for SOI_2 are different in shape and magnitude than those for SOI_1 and SOI_3. Since the head was not restrained by the side curtain air bag in SOI_2, the linear acceleration showed a lower peak and a longer duration than the remaining SOI conditions, resulting in a lower HIC15 value. Conversely, since there was a greater magnitude of angular rotation and angular velocity, the associated BRIC value was higher (Table D1 in Appendix D).

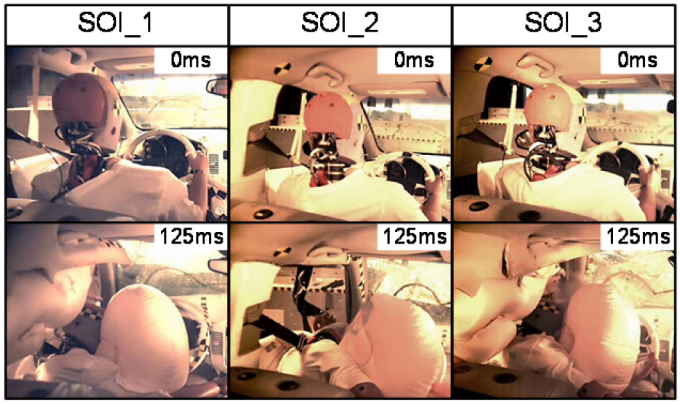


***Figure 17. Occupant initial position (0ms) and position of peak forward head excursion (125ms) in the SOI test condition.***

In the Oblique RMDB test condition, the timing of deployment of the inflatable restraints was more repeatable than in the SOI condition. As a result, the interaction of the THOR with the restraint system and the position of the head at the point of peak excursion were very similar in the three Oblique tests (Figure 20). In all three tests, the head first contacts the frontal air bag and begins to rotate roughly 45 degrees in the positive direction about the local Z-axis, then is restrained from further rotation by the side curtain air bag and retains this position throughout ride-down.

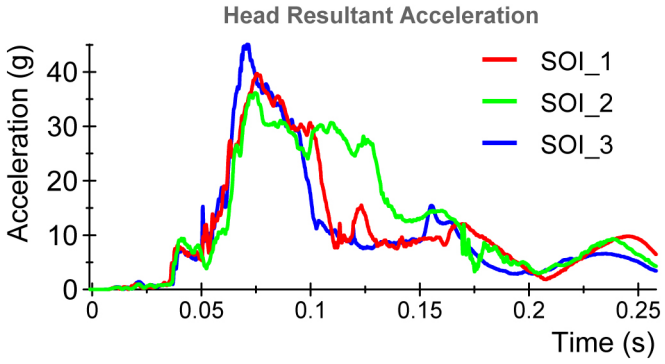


*Figure 18. Head resultant acceleration in the SOI test condition.*

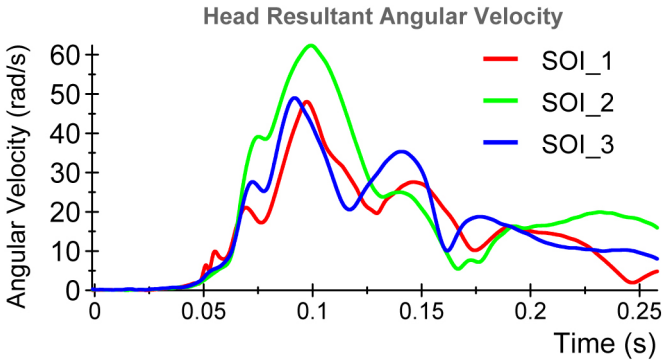


*Figure 19. Head resultant angular velocity in the SOI test condition.*

As suggested by the similar rotation of the head at the point of peak excursion, the angular velocity of the head in all three Oblique tests is nearly identical, especially to the point of peak forward excursion at 100 milliseconds (Figure 22). The linear acceleration of the head shows an overall similar shape and magnitude, except for a peak in the Oblique_2 condition between 60 and 70 milliseconds (Figure 21). The difference appears to stem from the fact that the side curtain air bag deploys 10 milliseconds later in the Oblique_2 condition than the other Oblique tests. In Oblique_1 and Oblique_3, the side curtain restraint is fully deployed when the head has translated forward and outboard far enough to contact it. However, in Oblique_2, the head has translated far enough forward and outboard that is impacted by the side curtain air bag as it deploys, resulting in a large magnitude spikes in the Head CG Y-and Z-axis accelerations. This difference leads to a higher calculated HIC15 value in the Oblique_2 condition, though this difference is not apparent in the HIC36 calculation (Table), most likely due to the relatively short duration of the difference.

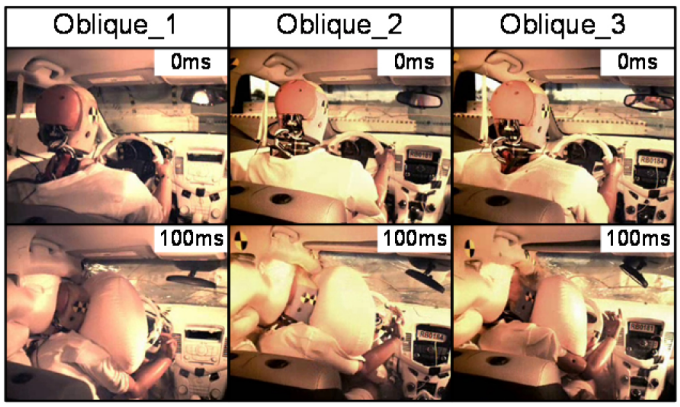


*Figure 20. Occupant initial position (0ms) and position of peak forward head excursion (100ms) in the Oblique test condition.*

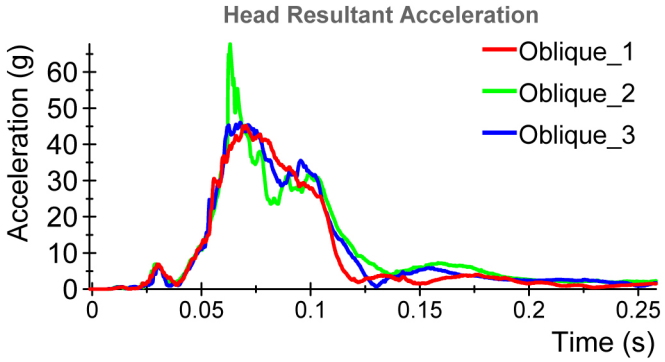


*Figure 21. Head resultant acceleration in the Oblique test condition.*

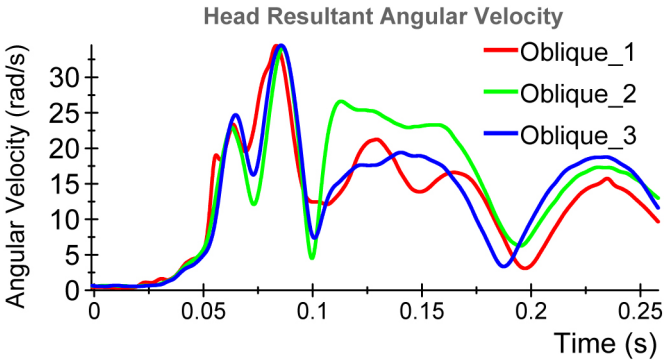


*Figure 22. Head resultant angular velocity in the Oblique test condition.*

## *Occupant injury assessment*

A set of injury assessment value (IAV) metrics were selected for the purposes of this comparison based on the available measurements and the existence of at least preliminary injury assessment reference values (IARVs) for the THOR ATD. Initially, event timing was included, but is not presented here because it was found that when the

calculations showed good agreement, the timing of the event showed as good or better agreement. For instance, when two HIC values differed by more than 20 percent, the timing of the event tended to be noticeably different. Presenting differences in both the timing of the head impact event and the calculated HIC values was thought to be redundant.

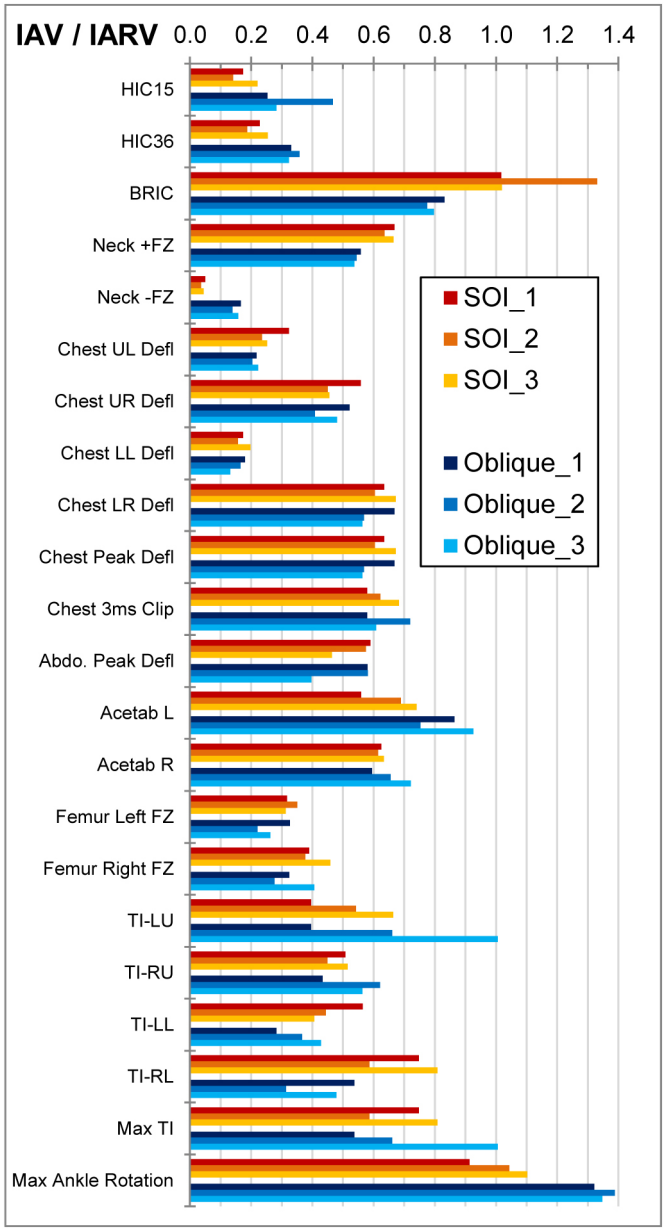


***Figure 23. Summary of the occupant response IAVs in the SOI (shades of red) and Oblique (shades of blue) repeated tests. IAVs are normalized by the associated IARV for the given metric.***

In order to further investigate the importance of the differences in injury assessment values (IAVs) for repeated tests, the IAVs were normalized by the associated IARVs for all of the injury metrics that were available to both the THOR ATD in the SOI and Oblique RMDB tests (Figure 23). A value of 1.0 would indicate that the measured value was equal to the injury assessment reference value, which in turn is associated with a given probability of a specific injury. As an overall assessment, the metrics that suggest the highest probability of injury include BRIC, acetabulum resultant force, tibia index, and ankle rotation. These metrics show good agreement with the field injury exposure [10], where the body regions with the highest incidence of injury were the knee/thigh/hip, chest, lower extremity, and head. One limitation to this assessment is that the relationship between injury risk and chest deflection as measured by the THOR ATD has not yet been developed.

The injury metrics that show the greatest dispersion among the repeated SOI and Oblique tests are HIC, BRIC, and Tibia Index. The differences in HIC and BRIC most likely result from differences in restraint timing, wherein each condition included a test with a delayed side curtain air bag deployment that influenced the result of one test, while the remaining two tests showed similar values. Tibia Index, on the other hand, did not follow this same pattern. Specifically, the upper left Tibia Index calculation resulted in three widely different values for each condition.

To quantify these differences, the coefficient of variation (CV) was calculated for each of the two groups (SOI and Oblique) for each IAV (Table 4). Overall, the CV values were considered acceptable (below 20%) aside from three exceptions. First, the HIC15 calculation in the Oblique condition showed a CV of 28%. This is likely due to the spike in head acceleration caused by late deployment of the side curtain air bag, as the remaining conditions showed very similar HIC15 values and the HIC36 showed a CV of only 4% for the same set of tests.

Second, the upper left Tibia Index had a CV of 21% and 36% for the SOI and Oblique groups, respectively. One possible reason for this large discrepancy was that instrumentation errors plagued the upper tibia load cell throughout these tests, resulting in questionable data measured for the upper tibia axial compressive force. Thus, the revised tibia index calculation relied on just the X- and Y-axis moments. It is also possible that difference in the recorded moments resulted from localized deformations of the instrument panel and interaction of the upper tibia with the knee bolster air bag.

Finally, the right lower Tibia Index in the Oblique condition showed a CV of 21%. The reason for the relatively high CV in this case appears to be related to instrumentation issues, as the quality of the data recorded by the tibia load cells and used to calculate tibia index (z-axis force, x- and y-axis moment) show irregularities that could be related to electrical interference in the load cell or the cables.

***Table 4. Summary of CV values for occupant IAV measures for the SOI and Oblique tsets. See appendix for a list including invividual values for each test.***

| Body Region | Metric | Location | SOI CV (%) | Oblique CV (%) |
|---|---|---|---|---|
| Head | HIC15 | Head CG | 18 | 28 |
| | HIC36 | Head CG | 12 | 4 |
| | BRIC | Head CG | 13 | 3 |
| Neck | Tension | UNLC | 2 | 2 |
| | Compression | UNLC | 13 | 7 |
| Chest | Deflection | UL | 14 | 4 |
| | Deflection | UR | 10 | 10 |
| | Deflection | LL | 10 | 13 |
| | Deflection | LR | 4 | 8 |
| | Deflection | Peak | 4 | 8 |
| | 3ms Clip | | 7 | 9 |
| Abdomen | Deflection | Peak | 10 | 17 |
| Acetabulum | Force (Res.) | Left | 12 | 8 |
| | Force (Res.) | Right | 1 | 8 |
| Femur | Force (Axial) | Left | 5 | 16 |
| | Force (Axial) | Right | 9 | 16 |
| Tibia | Tibia Index | LU | 21 | 36 |
| Tibia | Tibia Index | RU | 6 | 15 |
| Tibia | Tibia Index | LL | 14 | 17 |
| Tibia | Tibia Index | RL | 13 | 21 |
| Tibia | Tibia Index | Max | 13 | 27 |
| Ankle | [in/e]version | Left | 13 | 10 |
| Ankle | [in/e]version | Right | 3 | 17 |
| Ankle | [p/d]flexion | Left | 6 | 2 |
| Ankle | [p/d]flexion | Right | 4 | 6 |
| Ankle | Rotation | Max | 8 | 2 |
| Belt | Lap Belt | Max | 13 | 10 |
| | Shoulder Belt | Max | 2 | 6 |

## Repeatability Comparison

NHTSA's public vehicle database was searched for two or more of the same vehicle tested in the 56 kph full frontal or tested in the 60 kph 40 percent overlap test procedure. A list of tests used for this analysis is included in the Appendix E for the 56 kph full frontal an Appendix F for the 60 kph 40 percent overlap. Since many of the full frontal tests include only two data points per group, CVs were not calculated as these would not be particularly meaningful for these conditions. Instead, the difference in each pair or triplet of crash tests (indicating an identical vehicle, occupant, and test condition) was determined, and from all of the differences an average was calculated for each group.

For the purposes of this comparison, the tests are grouped into four categories: Full Frontal, ODB, SOI, and Oblique. The Full Frontal group, representing crash tests run at 56 kph into a full-width flat rigid barrier, consists of 12 pairs of tests and one set of three tests. In all of these tests, a 50$^{th}$ percentile male Hybrid III ATD was positioned in the driver's seat. The ODB group, representing crash tests run at 60 kph with a 40 percent offset into a fixed deformable barrier, consists of 10 groups of tests. The SOI and Oblique groups each included three vehicle tests, as described above.

### *Repeatability comparison: vehicle response*

This section compares the average bumper crush, toepan intrusions, and vehicle responses of the SOI and Oblique procedure to average of the Full Frontal and ODB test procedures.

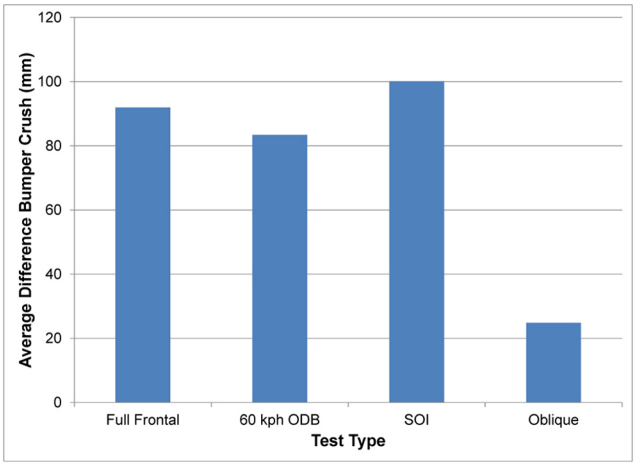


***Figure 24. Average difference in bumper crush at the left side of the vehicle***

Figure 24 shows that SOI average difference in bumper crush was similar to Full Frontal and 60 kph ODB tests. The oblique showed the lowest difference in bumper crush.

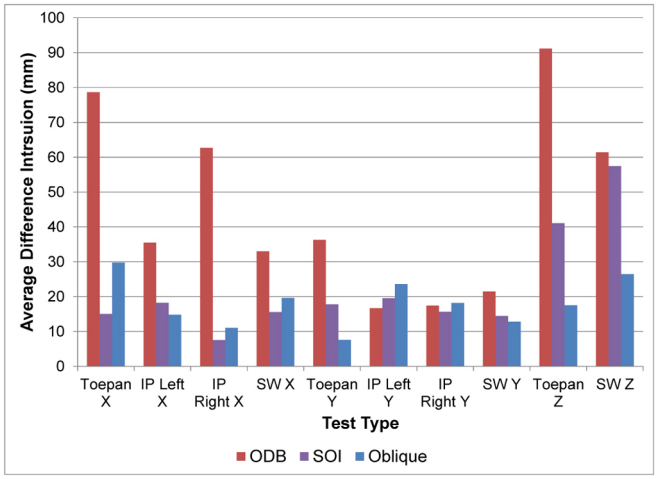


***Figure 25. Average differences in intrusions***

Since the toepan intrusion measurement procedures were not exactly the same for every test the intrusion point with the max X intrusion was used to calculate the differences. Figure 25 shows that both SOI and Oblique test procedure has similar if not better differences in occupant compartment intrusion when compared to the ODB tests

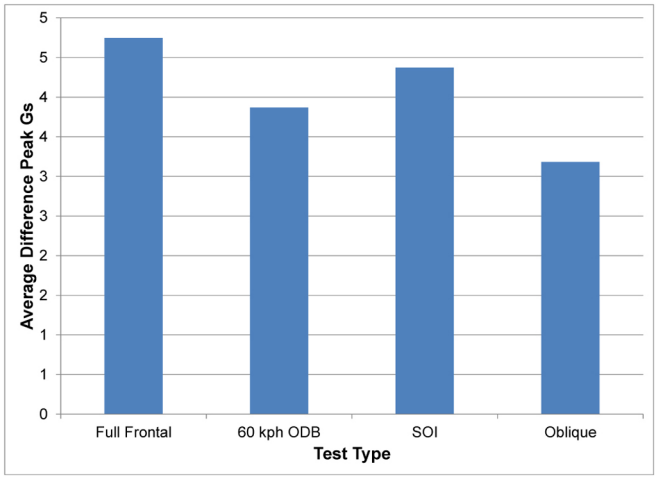


***Figure 26. Average difference for Peak Gs in the X-direction***

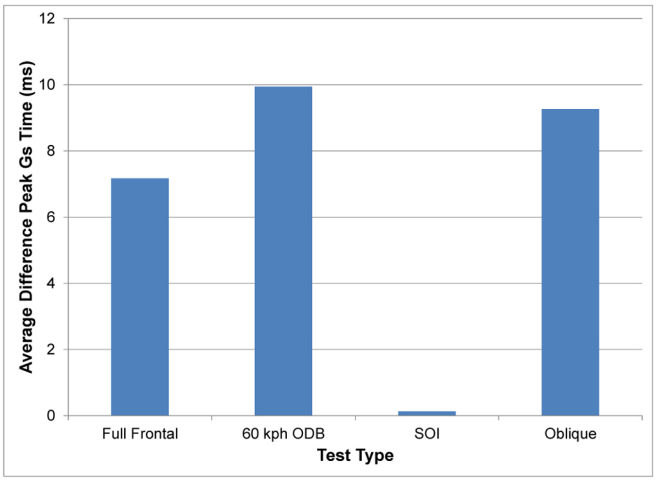


***Figure 27. Average difference in the time Peak Gs occurred***

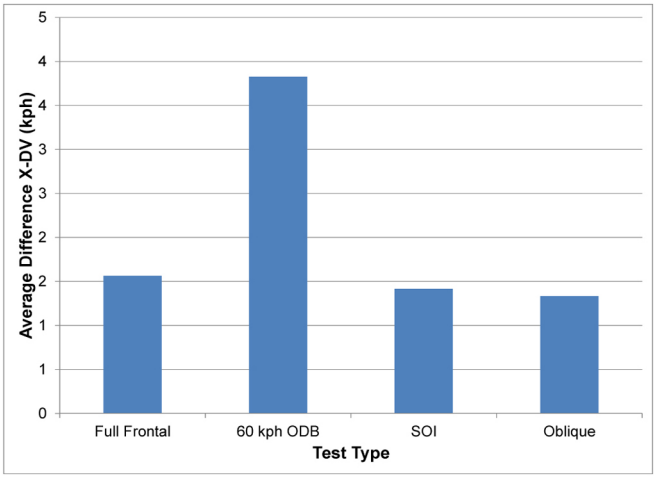


***Figure 28. Average difference in DV in the X-direction***

Figure 26 and Figure 27 and Figure 28 shows that the SOI and Oblique test procedure have similar results for the difference in peak Gs, the time peakc Gs occur, and total DV.

## *Repeatability comparison: occupant response*

To assess the relative repeatability of the occupant response, the set of injury assessment metrics presented earlier was refined to allow comparison to the full frontal crash tests and ODB crash tests that were conducted using a Hybrid III 5$^{th}$ or 50$^{th}$ percentile ATD in the driver's seat. For the Full Frontal and ODB groups, the differences in IAV values for each matching test was determined, and the average of all of the differences was taken. For the SOI and Oblique groups, maximum difference between any two of the tests was determined and compared to the average differences. The complete list is shown in Table D2 in appendix D. Figure 29 summarizes these data by presenting a normalized value consisting of, as the numerator, the average difference or maximum difference in IAV value between repeated tests, and as the denomonator, the maximum of these four values.

For 11 of the 15 IAVs, the maximum difference between any two repeated SOI or Oblique tests was lower than the average difference in the same IAV among the full frontal or ODB groups. These conditions are considered to have good repeatability since the test results are as repeatable as an existing crash test condition.

There was 1 IAV for which the maximum difference in the repeated SOI tests was greater than the average difference in the full frontal or ODB tests: pelvis acceleration. The difference in peak pelvis acceleration in the SOI tests stems from the X-axis acceleration for test SOI_1. While similar in shape and timing to the other SOI tests, is much different in magnitude (Figure 30). Since the lap belt loads were higher for this test (Figure 15), it was expected that the pelvis X-axis acceleration would be higher than the other SOI tests. This suggests the possibility of an instrumentation error, as neglecting this test results in difference in pelvis acceleration

of only 3.7g, which would be below the ODB average difference of 14g.

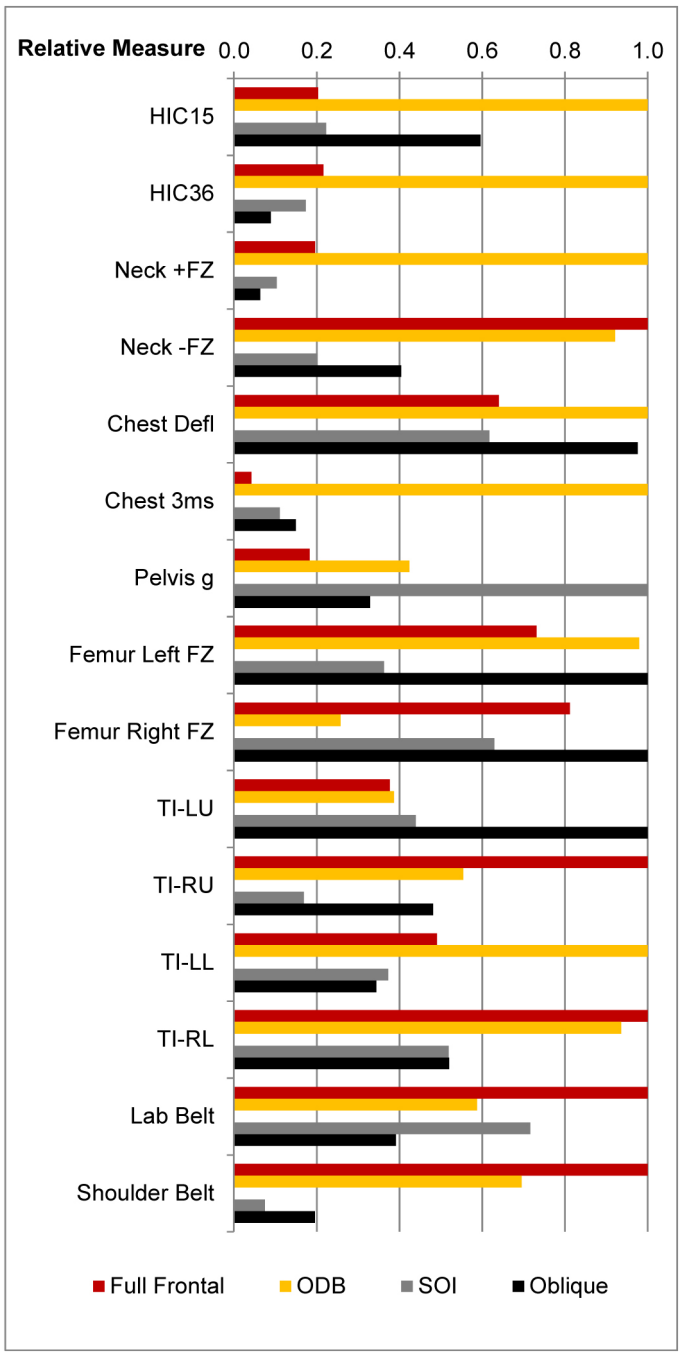


***Figure 29. Comparison of the average difference in IAVs for repeated tests to the maximum difference in repeated tests in the SOI and Oblique conditions.***

There were 3 IAVs for which the maximum difference in the repeated Oblique tests was greater than the average difference in the full frontal or ODB tests: left and right femur peak compressive force, and left upper Tibia Index. For the left femur, the maximum difference in the Oblique tests is very similar to the average difference in the ODB tests (949 N vs 930 N, respectively). For the right femur, the average difference in the full frontal tests is over 80 percent of the maximum difference in the repeated Oblique tests. As discussed earlier, differences in left upper Tibia Index were likely a result of faulty instrumentation.

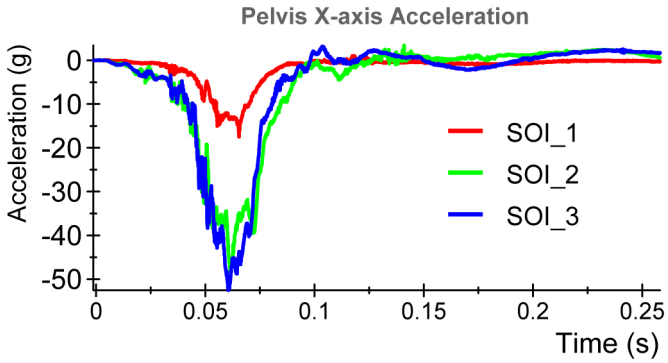


***Figure 30. Pelvis X-axis acceleration in the SOI tests.***

## DISCUSSION

Figure 6 showed that SOI_1 had more crush than SOI_2 and SOI_3. The Cruze 20 percent overlap target point ended up aligning with part of the frame (Figure 31). From this figure it can be seen that SOI_1 hit 3 mm to the left of the target point, while SOI_2 and SOI_3 hit approximately 25 mm to the right. This 28 mm more overlap may have caused the frame to deform differently than SOI_2 and SOI_3 (Figure 32). The frame for SOI_1 deformed inward and upward (Figure 32 (a)), while SOI_2 and SOI_3 the frame had a slight outward deformation and less deformation (Figure 32 (b)). Even though the bumper crush was different for SOI_1 the door post-test profile, toepan intrusion, left and right IP, and SW intrusion did not seem to be effected as much as expected, except in the Z-direction.

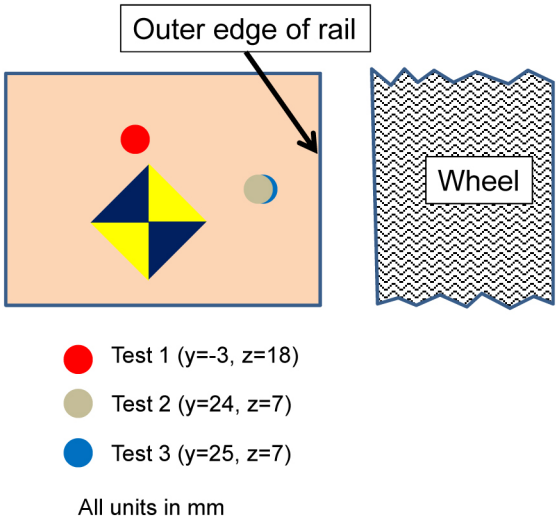


***Figure 31. Target point relative to the longitudinal rail***

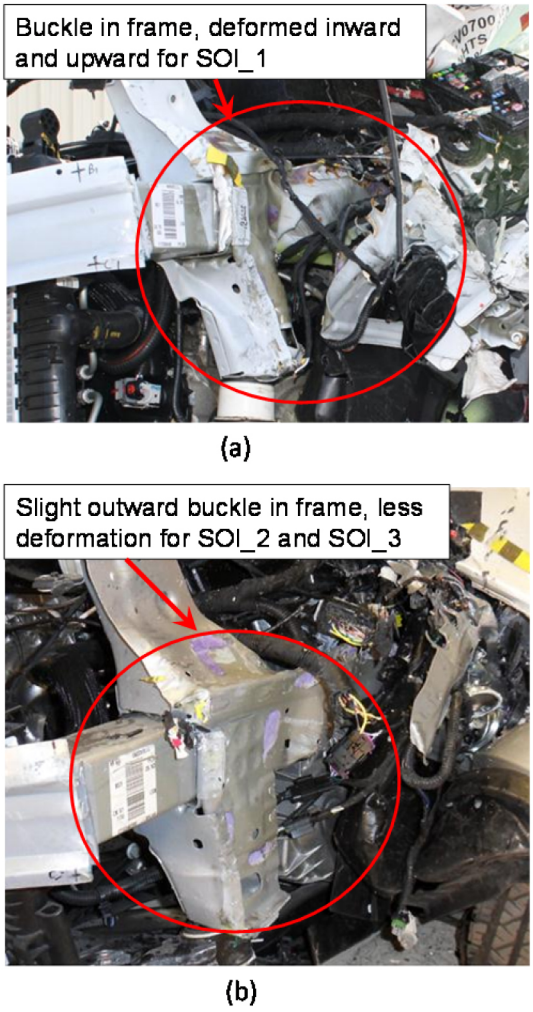


***Figure 32. Frame deformation comparison between SOI_1 and SOI_2 and SOI_3***

As measured by the response of the occupant, the SOI and Oblique test procedures showed similar repeatability. In both conditions, repeatability was generally acceptable, though there were noticeable differences in the response of the head and the tibia. As indicated earlier, the differences in head response are most likely related to the restraint deployment timing differences that occurred in the second test of each group. Especially in the Oblique condition, this finding suggests that the THOR ATD is sensitive to even minor changes in inflatable restraint deployment timing.

It is also noteworthy that the repeatability of the THOR ATD in these test conditions was comparable to that of the Hybrid III series of ATDs in full frontal and oblique test conditions. However, the repeatability and potentially the durability of the lower extremity hardware and instrumentation must be closely monitored in test conditions such as SOI and Oblique, where intrusions can occur at rates that exceed those of the hardware certification requirements.

With regard to vehicle repeatability, the categories where the largest differences were observed in the SOI and Oblique test conditions were toepan intrusion and steering wheel intrusion. In the case of toepan intrusion, the associated occupant response (revised tibia indices) also showed large differences. However, it is surprising that while the tibia measurements were among the least repeatable in the SOI and Oblique tests, the ankle rotations, especially plantar- and dorsiflexion, were among the most repeatable measures. This suggests that larger-scale intrusions may have been similar in order to impart similar gross motions on the feet of the occupant, while there may have been differences in localized loading (for instance, contact between the upper tibia and a different portion of the knee bolster air bag) that drove differences in the load paths to the lower extremity.

The steering wheel intrusion is an area where the occupant itself may have influenced the repeatability of the measured intrusion - and vice-versa. In test SOI_1, the steering wheel intrusion was 75 to 86 millimeters higher in the vehicle Z-axis direction than in the other SOI tests. Inspecting the post-test positions of the steering wheel rims (Figure 33), it appears that the steering wheel in SOI_1 was pushed upwards, towards the IP, and rotated about the vehicle Y-axis compared to the steering wheel in test SOI_3. One possibility for this change in post-test position is the interaction with the occupant in the driver's seat during the crash. Looking at the chest deflection measured by the THOR, the upper right compression in test SOI_1 is 20% higher in than the corresponding measurement in tests SOI_2 and SOI_3. A possible explanation for this difference could be that the occupant in SOI_1 was positioned slightly farther inboard (note that the head was 28 millimeters farther inboard in this test), which could have resulted in more interaction between the steering wheel rim and the upper right chest at the point of peak forward occupant excursion. The side-view onboard high-speed video suggests that this difference is possible, but it is obfuscated by the deployed frontal air bag.

It is difficult to compare this current repeatability study to previous research that has addressed the repeatability of vehicle crash test procedures. Previous repeatability analyses have defined a test procedure to be repeatable if the score or rating of the vehicle does not change from test to test. Since the SOI and Oblique procedures are part of a research program, insufficient testing and regulatory analysis has been carried out to determine what the rating scheme would be. In lieu of the change-of-rating assessment method, repeatability was quantified herein using CV and by comparing the magnitude of test-to-test differences in the current SOI and Oblique tests with average differences in previous full-frontal and ODB tests. As such, this comparison is not biased by rating schemes that may have large allowances and nonuniform ranges for specific injury metrics. For instance, the New Car Assessment Program (NCAP) ratings are based on varied probability ranges (0.2 for 2 stars, 0.05 for 3 and 4 stars) which are calculated from nonlinear probability functions [11]. As an example, three repeated tests could have $HIC_{15}$ values of 100, 300, and 500 (CV = 54%), and

these might be deemed repeatable since the same rating would result.

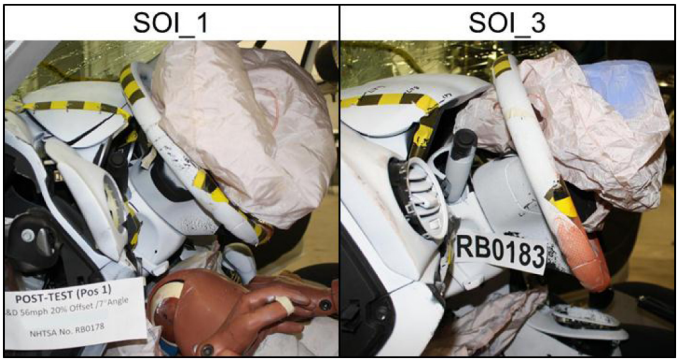


***Figure 33. Post-test steering wheel position difference between SOI_1 and SOI_3.***

# LIMITATIONS

The analysis of SOI and Oblique repeatability was limited to three tests in each condition on a single vehicle model. On the same note, although the base model was specified during the purchase of all six vehicles used in this study, the first vehicle in each group was configured with an automatic transmission, while the second and third vehicles had manual transmissions. Differences in the transmission geometry and mass may have led to differences in the vehicle acceleration pulses as well as intrusions into the IP and toepan. This is most apparent in the X-axis accelerations (Figure 10) for both test procedures, where the first vehicle in each group demonstrates small differences in peak and shape. It should also be noted that the three vehicles in each test mode were not consecutively manufactured as has been the case in previous studies. This observation suggests that had the vehicles been equipped with identical powertrains and had been sequentially manufactured, the repeatability in vehicle response may have been improved.

Comparing the results from the current SOI and Oblique tests with those from full frontal and ODB tests has several limitations. The existing tests were not run specifically for this study, so there was not necessarily an effort to match the test vehicles directly (for instance, there is no guarantee that the same wheel type was used in all test pairs), and the amount of information available to confirm this is limited by the quality of existing test reports. However, these were verified to the best of the authors' ability, and tests with known vehicle redesigns between the paired tests were excluded. Also, the procedure used to measure intrusion, along with the coordinate system in which it was measured, may not have been the same for all the 60 kph ODB tests.

# CONCLUSIONS

The following conclusions are based on one vehicle model and three tests in each test condition. The results may be different for a different make and model or if more tests were performed.

**1).** The repeatability of the SOI condition, even though it was expected to be less repeatable due to having less involvement with the longitudinal rail of the impacted vehicle, was not markedly lower than that of the Oblique condition.

**2).** The differences that did occur in the occupant response as measured by the THOR ATD in the driver's seat primarily resulted from differences in structural intrusions into the occupant compartment and from differences in deployment times of the inflatable restraints, primarily the side curtain air bags.

**3).** The repeatability of the SOI and Oblique conditions was equivalent to the repeatability demonstrated in existing vehicle tests in the full frontal and offset deformable barrier crash test conditions.

# REFERENCES

1. Saunders, J., Craig, M., and Parent, D., "Moving Deformable Barrier Test Procedure for Evaluating Small Overlap/Oblique Crashes," *SAE Int. J. Commer. Veh.* 5(1):172-195, 2012, doi: 10.4271/2012-01-0577.
2. Meyerson, S., Zuby D., and Lund Adrian. "Repeatability of frontal offset crash tests." 15th International Technical Conference on the Enhanced Safety of Vehicles, Melbourne, Australia. 1996.
3. Ridella, S., Parent, D., "Modifications to Improve the Durability, Usability, and Biofidelity of the THOR-NT Dummy," 22nd ESV Conference, Paper No. 11-0312, 2011.
4. Eppinger, R., Sun, E., Bandak, F., Haffner, M., Khaewpong, N., Maltese, M., Kuppa, S., Nguyen, T., Takhounts, E., Tannous, R., Zhang, A., Saul, R., "Development of Improved Injury Criteria for the Assessment of Advanced Automotive Restraint Systems - II," National Highway Traffic Safety Administration, Washington D.C., November 1999.
5. Takhounts, E.G., Hasija, V., Ridella, S.A., Rowson, S., Duma, S., "Kinematic Rotational Brain Injury Criterion (BRIC)," 22nd ESV Conference, Paper No. 11-0263, 2011.
6. Dibb, A., Nightingale, R., Chauncey, V., Fronheiser, L., Tran, L., Ottaviano, D., Myers B., "Comparative Structural Neck Responses of the THOR-NT, Hybrid III, and Human in Combined Tension-Bending and Pure Bending," Stapp Car Crash Journal, 50: 567-581, 2006.
7. Rupp, J.D., Flannagan, C.A., Kuppa, S.M., "Development of an injury risk curve for the hip for use in frontal impact crash testing," Journal of Biomechanics 34(3):527-531, 2010.
8. Martin, P.G., Scarboro, M., "THOR-NT: Hip Injury Potential In Narrow Offset And Oblique Frontal Crashes," 22nd ESV Conference, Paper No. 11-0234, 2011.
9. Kuppa, S., Wang, J., Haffner, M., Eppinger, R., "Lower Extremity Injuries and Associated Injury Criteria," 17th ESV Conference, Paper No. 457, 2001.
10. Rudd, R., Scarboro, M., Saunders, J., "Injury Analysis of Real-World Small Overlap and Oblique Frontal Crashes," 22nd ESV Conference, Paper No. 11-0384, 2011.
11. National Highway Traffic Safety Administration, "Consumer Information; New Car Assessment Program," Docket No. NHTSA-2006-26555, Document No. 0114, 2006.

# APPENDIX

## APPENDIX A - BUMPER BEAM MEASUREMENTS PROCEDURE

The following is the procedure to measure the bumper beam:

**a).** Expose the front bumper beam

**b).** Mark the both ends of the upper part of the bumper beam.

**c).** Mark the upper part of the bumper beam with four (4) equally spaced points between the end points. Point 1 shall be at the driver side end of the bumper beam. Point 6 shall be at the passenger side end of the bumper beam.

## APPENDIX B - DOOR PROFILE MEASUREMENTS PROCEDURE

The following is the procedure to measure the door profile pre and post-test (Figure 3):

**a).** On the driver's door sill mark a point at the intersection of the A post and window sill (point 1). All points should be half way between the outer and inner vehiclre door sill.

**b).** Mark a point at the intersection of the roof rail and the B post (point 16).

**c).** Mark a point at the intersection of the B post and the door sill (point 22).

**d).** Mark a point at the intersection of the A post and the door sill (point 29).

**e).** Mark 14 evenly spaced points between points 1 and 16. (A tape measure can be used to mark these points).

**f).** Mark 5 evenly spaced points between points 16 and 22. (A tape measure can be used to mark these points).

**g).** Mark 5 evenly spaced points between points 22 and 29. (A tape measure can be used to mark these points).

**h).** Mark 3 evenly spaced points between points 29 and 1. (A tape measure can be used to mark these points).

## APPENDIX C - INTERIOR POINTS MEASUREMENTS PROCEDURE

**Interior intrusion:** Procedure to map the 4 by 5 matrix toepan and floorpan intrusion points Figure 4):

**1.** Locate and mark point D1 (column D row 1): Project a line 45 degrees (from the horizontal) down and forward from the center of the top accelerometer pedal in the x-z plane until the line intersects the interior of the vehicle. Mark this point by cutting a small “v” in the carpet and underlying padding and peeling back and exposing the floor. The carpet and padding are then refitted prior to crash.

**2.** ST plane: The ST plane is a y-z plane that passes through the front edge of the right seat track.

**3.** AP1 plane: The AP1 plane is a y-z plane that passes through point D1.

**4.** AP2 plane: The AP2 plane is an x-z plane that passes through point D1.

**5.** AP3 plane: The AP3 plane is an x-y plane that passes through point D1.

**6.** MP plane: The MP plane is a y-z plane located halfway between the ST plane and AP1 plane.

**7.** CF plane: The CF plane is an x-z plane that passes through the center of the footrest. If there is no visible footrest, locate the x-z plane to pass through a point located 64 mm measured along the MP plane in the y-direction from the intersection of the door sill and floorboard.

**8.** BP plane: The BP plane is an x-z plane that passes through the center of the brake pedal.

**9.** TP plane: The TP plane is a y-z plane at the intersection of the BP plane and the intersection of the toe pan and floorboard.

**10.** Column A is at the intersection of the vehicle and the CF plane.

**11.** Column D is at the intersection of the vehicle and the AP2 plane.

**12.** Row 1 is at the intersection of the vehicle and the AP3 plane.

**13.** Row 3 is at the intersection of the vehicle and the TP plane.

**14.** Row 5 is at the intersection of the vehicle and MP plane.

**15.** Columns B and C are evenly spaced between Columns A and D.

**16.** Row 2 is evenly spaced between Row 1 and Row 3.

**17.** Row 4 is evenly spaced between Row 3 and Row 5.

# APPENDIX D - INJURY ASSESSMENT VALUES

***Table D1. Injury Assessment Values for the THOR ATD in the driver's seat in the SOI and Oblique RMDB tests***

| Body Region | Metric | Location | Units | Ref. | SOI | | | | Oblique | | | |
|---|---|---|---|---|---|---|---|---|---|---|---|---|
| | | | | | 1 [7432] | 2 [7773] | 3 [7867] | CV (%) | 1 [7431] | 2 [7852] | 3 [7851] | CV (%) |
| **Head** | HIC15 | Head CG | | 700 | 122 | 99 | 155 | 18 | 177 | 198 | 327 | 28 |
| | HIC36 | Head CG | | 1000 | 228 | 187 | 254 | 12 | 331 | 324 | 358 | 4 |
| | BRIC | Head CG | | 0.89 | 0.91 | 1.18 | 0.91 | 13 | 0.74 | 0.71 | 0.69 | 3 |
| **Neck** | Tension | UNLC | N | 2520 | 1684 | 1602 | 1675 | 2 | 1406 | 1355 | 1372 | 2 |
| | Compression | UNLC | N | -3640 | -183 | -134 | -163 | 13 | -605 | -573 | -507 | 7 |
| **Chest** | Deflection | UL | mm | 63 | 20.4 | 14.9 | 15.9 | 14 | 13.7 | 12.8 | 14.1 | 4 |
| | Deflection | UR | mm | 63 | 35.2 | 28.3 | 28.7 | 10 | 32.9 | 25.7 | 30.3 | 10 |
| | Deflection | LL | mm | 63 | 11.0 | 9.9 | 12.5 | 10 | 11.3 | 10.4 | 8.3 | 13 |
| | Deflection | LR | mm | 63 | 40.0 | 38.1 | 42.4 | 4 | 42.1 | 35.9 | 35.5 | 8 |
| | Deflection | Peak | mm | 63 | 40 | 38 | 42 | 4 | 42 | 36 | 36 | 8 |
| | 3ms Clip | | G | 60 | 34.7 | 37.3 | 41.0 | 7 | 34.8 | 36.5 | 43.2 | 9 |
| **Abdomen** | Deflection | Peak | mm | 90 | 53.0 | 51.8 | 41.7 | 10 | 52.3 | 52.4 | 35.7 | 17 |
| **Acetabulum** | Force (Res.) | Left | N | 3316 | 1853 | 2284 | 2455 | 12 | 2866 | 2499 | 3069 | 8 |
| | Force (Res.) | Right | N | 3316 | 2075 | 2039 | 2101 | 1 | 1972 | 2176 | 2394 | 8 |
| **Femur** | Force (Axial) | Left | N | 9040 | -2866 | -3171 | -2827 | 5 | -2950 | -2373 | -2000 | 16 |
| | Force (Axial) | Right | N | 9040 | -3523 | -3410 | -4150 | 9 | -2932 | -3669 | -2494 | 16 |
| **Tibia** | Tibia Index | LU | | 1.16 | 0.46 | 0.63 | 0.77 | 21 | 0.46 | 1.17 | 0.77 | 36 |
| **Tibia** | Tibia Index | RU | | 1.16 | 0.59 | 0.52 | 0.60 | 6 | 0.50 | 0.65 | 0.72 | 15 |
| **Tibia** | Tibia Index | LL | | 1.16 | 0.66 | 0.52 | 0.47 | 14 | 0.33 | 0.50 | 0.43 | 17 |
| **Tibia** | Tibia Index | RL | | 1.16 | 0.87 | 0.68 | 0.94 | 13 | 0.62 | 0.55 | 0.36 | 21 |
| **Tibia** | Tibia Index | Max | | 1.16 | 0.87 | 0.68 | 0.94 | 13 | 0.62 | 1.17 | 0.77 | 27 |
| **Ankle** | [in/e]version | Left | deg | 35 | 27.5 | 30.5 | 37.3 | 13 | 30.1 | 38.5 | 32.6 | 10 |
| **Ankle** | [in/e]version | Right | deg | 35 | IM | 36.5 | 38.6 | 3 | 38.7 | 25.4 | 33.0 | 17 |
| **Ankle** | [p/d]flexion | Left | deg | 35 | 32.0 | 30.5 | 34.9 | 6 | 46.2 | 47.1 | 48.6 | 2 |
| **Ankle** | [p/d]flexion | Right | deg | 35 | IM | 19.5 | 21.1 | 4 | 26.7 | 23.5 | 24.1 | 6 |
| **Ankle** | Rotation | Max | deg | 35 | 32.0 | 36.5 | 38.6 | 8 | 46.2 | 47.1 | 48.6 | 2 |
| **Belt** | Lap Belt | Max | N | NA | 5435 | 3939 | 4486 | 13 | 3202 | 4020 | 3992 | 10 |
| | Shoulder Belt | Max | N | NA | 3430 | 3253 | 3388 | 2 | 3500 | 3039 | 3229 | 6 |

***Table D2. Comparison of occupant response metrics between repeated Full Frontal, ODB, SOI, and Oblique tests.***

| Body Region | Metric | Location | Units | Ref. | Full Frontal Max | Full Frontal Avg Diff | ODB Max | ODB Avg Diff | SOI Max | SOI Max Diff | Oblique Max | Oblique Max Diff |
|---|---|---|---|---|---|---|---|---|---|---|---|---|
| Head | HIC15 | Head CG | | 700 | 619 | 51 | 1324 | 252 | 155 | 56 | 327 | 150 |
| | HIC36 | Head CG | | 1000 | 908 | 84 | 1920 | 388 | 254 | 67 | 358 | 35 |
| Neck | Tension | UNLC | N | 2520 | 2388 | 155 | 3717 | 789 | 1684 | 82 | 1406 | 50 |
| | Compression | UNLC | N | -3640 | 1340 | 243 | 1556 | 224 | 183 | 49 | 605 | 98 |
| Chest | Deflection | Peak | mm | 63 | 46 | 4 | 36 | 7 | 42 | 4 | 43 | 7 |
| | 3ms Clip | | g | 60 | 60 | 2 | 491 | 56 | 41 | 6 | 43 | 8 |
| Pelvis | Acceleration | Peak | g | NA | 96 | 6 | 68 | 14 | 55 | 34 | 61 | 11 |
| Femur | Force (Axial) | Left | N | 9040 | 7292 | 695 | 7266 | 930 | 3171 | 344 | 2950 | 949 |
| | Force (Axial) | Right | N | 9040 | 6692 | 954 | 4939 | 303 | 4150 | 740 | 3669 | 1175 |
| Tibia | Tibia Index | LU | | 1.16 | 0.83 | 0.27 | 2.23 | 0.27 | 0.77 | 0.31 | 1.17 | 0.71 |
| Tibia | Tibia Index | RU | | 1.16 | 1.79 | 0.45 | 1.17 | 0.25 | 0.60 | 0.08 | 0.72 | 0.22 |
| Tibia | Tibia Index | LL | | 1.16 | 0.75 | 0.24 | 1.93 | 0.49 | 0.66 | 0.18 | 0.50 | 0.17 |
| Tibia | Tibia Index | RL | | 1.16 | 1.98 | 0.50 | 1.27 | 0.47 | 0.94 | 0.26 | 0.62 | 0.26 |
| Belt | Lap Belt | Max | N | NA | 9502 | 2088 | 5187 | 1227 | 5435 | 1496 | 4020 | 818 |
| | Shoulder Belt | Max | N | NA | 15575 | 2355 | 7967 | 1639 | 3430 | 177 | 3500 | 460 |

# APPENDIX E - 56 KPH FULL FRONTAL CRASH TESTS

The following table shows the 56 kph full frontal crash tests used for analysis.

| NHTSA Test Number | MAKED | MODELD | YEAR |
|---|---|---|---|
| 4244 | CHEVROLET | TRAILBLAZER | 2002 |
| 5036 | CHEVROLET | TRAILBLAZER | 2002 |
| 5061 | DODGE | RAM | 2002 |
| 4240 | DODGE | RAM1500 | 2002 |
| 5073 | TOYOTA | TUNDRA | 2002 |
| 3915 | TOYOTA | TUNDRA | 2002 |
| 5711 | CHEVROLET | SILVERADO | 2003 |
| 4472 | CHEVROLET | SILVERADO | 2003 |
| 5273 | HONDA | ODYSSEY | 2005 |
| 5714 | HONDA | ODYSSEY | 2005 |
| 5160 | TOYOTA | COROLLA | 2005 |
| 5388 | TOYOTA | COROLLA | 2005 |
| 6258 | CADILLAC | CTS | 2008 |
| 6271 | CADILLAC | CTS | 2008 |
| 6724 | HONDA | INSIGHT | 2010 |
| 6729 | HONDA | INSIGHT | 2010 |
| 6759 | HYUNDAI | GENESIS | 2010 |
| 6764 | HYUNDAI | GENESIS | 2010 |
| 6736 | KIA | FORTE | 2010 |
| 6753 | KIA | FORTE | 2010 |
| 6766 | KIA | FORTE | 2010 |
| 6641 | KIA | SOUL | 2010 |
| 6655 | KIA | SOUL | 2010 |
| 6642 | LEXUS | RX350 | 2010 |
| 6643 | LEXUS | RX350 | 2010 |
| 6647 | MAZDA | MAZDA3 | 2010 |
| 6658 | MAZDA | MAZDA3 | 2010 |

# APPENDIX F - 60 KPH 40 PERCENT OFFSET FIXED DEFORMABLE BARRIER TESTS

**60 kph 40 Percent Overlap Fixed Deformable Barrier:** The following table shows the 60 kph 40 Percent Overlap Fixed Deformable Barrier crash tests used for analysis.

| NHTSA Test Number | MAKED | MODELD | YEAR |
|---|---|---|---|
| 2675 | FORD | TAURUS | 1996 |
| 2677 | FORD | TAURUS | 1996 |
| 2665 | TOYOTA | CAMRY | 1996 |
| 3664 | TOYOTA | CAMRY | 1996 |
| 2678 | TOYOTA | CAMRY | 1996 |
| 3459 | TOYOTA | CAMRY | 1996 |
| 2963 | CHEVROLET | VENTURE | 1998 |
| 2902 | CHEVROLET | VENTURE | 1998 |
| 2964 | DODGE | NEON | 1998 |
| 3667 | DODGE | NEON | 1998 |
| 2897 | DODGE | NEON | 1998 |
| 3466 | DODGE | NEON | 1998 |
| 2912 | FORD | CONTOUR | 1998 |
| 2906 | FORD | CONTOUR | 1998 |
| 3442 | CHEVROLET | TAHOE | 2000 |
| 3855 | CHEVROLET | TAHOE | 2000 |
| 3666 | NISSAN | ALTIMA | 2000 |
| 3909 | NISSAN | ALTIMA | 2000 |
| 3849 | NISSAN | QUEST | 2000 |
| 3856 | NISSAN | QUEST | 2000 |
| 3854 | NISSAN | QUEST | 2000 |
| 3857 | NISSAN | QUEST | 2000 |
| 3665 | SUBARU | LEGACY | 2000 |
| 3907 | SUBARU | LEGACY | 2000 |
| 4440 | NISSAN | ALTIMA | 2002 |
| 4461 | NISSAN | ALTIMA | 2002 |
| 4724 | NISSAN | ALTIMA | 2002 |
| 4725 | NISSAN | ALTIMA | 2002 |
| 4797 | NISSAN | ALTIMA | 2002 |